HHS Public Access

Author manuscript

J Inherit Metab Dis. Author manuscript; available in PMC 2020 September 01.

Published in final edited form as:

J Inherit Metab Dis. 2019 September ; 42(5): 998–1007. doi:10.1002/jimd.12110.

A Novel Phosphoglucomutase-deficient Mouse Model Reveals Aberrant Glycosylation and Early Embryonic Lethality

B Balakrishnan[1], **J Verheijen**[2], **A Lupo**[1], **K Raymond**[2], **CT Turgeon**[2], **Y Yang**[1], **KL Carter**[3], **KJ Whitehead**[3], **T Kozicz**[2], **E Morava**[2], **K Lai**[1,*]

[1]Department of Pediatrics, University of Utah School of Medicine, Salt Lake City, Utah

[2]Center for Individualized Medicine, Department of Clinical Genomics, and Biochemical Genetics Laboratory, Mayo Clinic, Rochester, Minnesota

[3]Small Animal Ultrasound Core Facility, University of Utah School of Medicine, Salt Lake City, Utah

Abstract

Patients with phosphoglucomutase (PGM1) deficiency, a congenital disorder of glycosylation (CDG) suffer from multiple disease phenotypes. Midline cleft defects are present at birth. Overtime, additional clinical phenotypes, which include severe hypoglycemia, hepatopathy, growth retardation, hormonal deficiencies, hemostatic anomalies, frequently lethal, early-onset of dilated cardiomyopathy (DCM) and myopathy emerge, reflecting the central roles of the enzyme in (glycogen) metabolism and glycosylation. To delineate the pathophysiology of the tissue-specific disease phenotypes, we constructed a constitutive *Pgm2* (mouse ortholog of human *PGM1*)-knockout (KO) mouse model using CRISPR-Cas9 technology. After multiple crosses between heterozygous parents, we were unable to identify homozygous life births in 78 newborn pups (p = 1.59897E-06), suggesting an embryonic lethality phenotype in the homozygotes.

*Corresponding Author: Kent Lai, Division of Medical Genetics, Department of Pediatrics, University of Utah School of Medicine, 295 Chipeta Way, Salt Lake City, Utah, U.S.A. 84108, kent.lai@hsc.utah.edu.

Details of the contributions of individual authors:
Bijina Balakrishnan – Planning and Performance of the Experiments, Interpretation of the Results, and Composition of the Manuscript.
Jan Verheijen - Performance of the Experiments and Interpretation of the Results.
Arielle Lupo - Performance of the Experiments.
Coleman Turgeon - Performance of the Experiments.
Kimiyo Raymond – Reviewing Experimental data.
Yueqin Yang - Performance of the Experiments.
Kandis L Carter - Performance of the Experiments.
Kevin Whitehead - Planning of the Experiments.
Tamas Kozicz - Planning of the Experiments, Interpretation of the Results, and Composition of the Manuscript
Eva Morava - Planning of the Experiments, Interpretation of the Results, and Composition of the Manuscript
Kent Lai - Planning and Performance of the Experiments, Interpretation of the Results, and Composition of the Manuscript.

A competing interest statement
No competing interest to declare.

Details of ethics approval
This research does not involve human subjects and therefore, IRB approval is not required.

A patient consent statement
Not Applicable.

Documentation of approval from the Institutional Committee for Care and Use of Laboratory Animals (or comparable committee)
This research is conducted in strict adherence to protocol approved by the ICAUC of University of Utah.

Ultrasound studies of the course of pregnancy confirmed Pgm2-deficient pups succumb before E9.5. Oral galactose supplementation (9mg/ml drinking water) did not rescue the lethality. Biochemical studies of tissues and skin fibroblasts harvested from heterozygous animals confirmed reduced Pgm2 enzyme activity and abundance, but no change in glycogen content. However, glycomics analyses in serum revealed an abnormal glycosylation pattern in the *Pgm2*$^{+/-}$ animals, similar to that seen in PGM1-CDG.

Keywords

Congenital disorders of Glycosylation; Phosphoglucomutase1 deficiency; Inborn errors of metabolism; Embryonic lethality; Aberrant *N*-linked glycosylation; Galactose supplementation

Introduction

Phosphoglucomutase 1 (PGM1) catalyzes the interconversion of glucose-1 phosphate (Glc-1P) and glucose-6 phosphate (Glc-6P) and therefore, it plays a fundamental role in glycolysis, glycogenesis, and glycogenolysis (Beamer 2015). Consequently, inherited deficiency of PGM1 in humans has previously been identified as Glycogen Storage Disorder (**GSD**) Type 14, which resulted from deleterious recessive variants in the *PGM1* genes (Voermans et al. 2017; Ondruskova et al. 2014). Yet, PGM1 deficiency is increasingly recognized as a congenital disorder of glycosylation **(CDG)**, where reduced *N*-linked glycosylation in the endoplasmic reticulum (ER) and Golgi is observed, resulting in both missing and truncated glycans (mixed type I and type II glycosylation defects) (Perez et al. 2013; Jaeken 2011; Kucukcongar et al. 2015; Ondruskova et al. 2014).

At birth, affected patients have frequent malformations in the spectrum of bifid uvula, cleft palate, and Pierre-Robin sequence. The liver, the skeletomuscular system, endocrine and coagulation systems get all involved overtime, but the most life-threatening complication is the early-onset dilated cardiomyopathy (**DCM**), reflecting the central roles of the enzyme in glycogen metabolism and glycosylation (Timal et al. 2012; Tegtmeyer et al. 2014; Loewenthal et al. 2015; Stojkovic et al. 2009) (Fig. 1). Recently, it has been shown that oral D-galactose supplementation in a growing cohort of patients with PGM1 deficiency improved serum transferrin hypoglycosylation, liver function, endocrine abnormalities, and reduced the frequency of hypoglycemic episodes (Morava 2014; Wong et al. 2017; Tegtmeyer et al. 2014; Radenkovic et al. 2019). However, not all clinical abnormalities were corrected at the dosage used. A better understanding of the pathophysiology of PGM1 deficiency is needed to enable the development of more effective therapies for this disorder. As human PGM1 and mouse Pgm2 are 97.7% identical at the amino acid level and catalyze the same reactions, while the mouse Pgm1 converts ribose-1-phosphate/deoxyribose-1-phosphate to the corresponding 5-phosphopentose (Shows, Ruddle, and Roderick 1969), we examined the disruption of the *Pgm2* gene in the mouse.

Materials and Methods

Construction of the constitutive Pgm2-KO mouse model

Construction and characterization of the *Pgm2-KO* were conducted in accordance to the approved IACUC protocol.

Pgm2-KO mice were generated using the CRISPR/Cas9 approach at the Transgenic and Gene Targeting Mouse Core and the Mutation Generation and Detection Core, University of Utah. Guide RNAs (gRNAs) targeting exon 2 and exon 3 of *Pgm2* were designed using CRISPOR (http://crispor.tefor.net, PMID: 27380939) and off-target sites were predicted using (http://casot.cbi.pku.edu.cn PMID: 24389662). gRNA N(20) sequences used are as follows; CGAGGTCTACCTTCAAGTCA and GGATGATGCAAGATACGGCA. The gRNAs were synthesized by making PCR templates that were transcribed with T7 RNA polymerase (Lin et al. 2014).

Super-ovulated C57Bl6/J embryos were harvested at E 0.5, treated with hyaluronidase in M2 medium, and incubated in M16 medium under oil. CRISPR reagents were injected into the pronucleus of fertilized embryos. Two guide RNA's; PGM2-E2-S10 and PGM2-E3-S13 were diluted to 20 ng/μl each along with Cas9 protein at 20 ng/μl in RNase free water. Injected embryos were implanted into the oviduct of 0.5-day pseudo pregnant females and allowed to be born naturally. Pups were ear clipped for genotyping at p14.

TA Cloning and DNA sequencing

PCR primer sequences used in direct sequencing were as follows: Exon 2 site: Forward: tcctagATTGGTCGCCTGGT; Reverse: CCTGGATTATGGCTGGCTGT Exon 3 site: Forward: GATTGCTGAGTGCTGGGTTG; Reverse: GGGCAGGGACAGTAACATGC.

PCR products from genomic DNA were cloned into pSC-A (Stratagene, Cedar Creek, TX). Plasmid DNA was prepared and sequenced using the BigDye Terminator v3.1 Cycle Sequencing Kit (Applied Biosystems) with M13 forward or reverse primers.

PCR-based genotyping and Restriction Fragment Length Polymorphism (RFLP)

Germline transmission of mutant alleles in subsequent generations was confirmed by a rapid PCR-based genotyping protocol and RFLP.

The sequences for the PCR primers used are:

Forward: TGCCTTACAGCACCTCAGTG

Reverse: AACCCAGCACTCAGCAATCC

The PCR product is digested with *Bce*AI (New England Biolabs cat. no. R0623L) and resolved by a 2 % agarose gel.

Ultrasound studies

Immediately after mating began, six female mice were monitored by ultrasound daily. Images were acquired with B-mode, and color Doppler modes using a Vevo 2100 high frequency ultrasound machine (VisualSonics) and a MS700 40MHz probe. Scan time was approximately 45 minutes to identify number and location of all embryos and obtain images. The timing of the pregnancies was determined based on the developmental stages revealed by the images. As soon as deaths were noted, the pregnant mouse was euthanized and embryos dissected for genotyping.

Timed matings

Heterozygous *Pgm2*$^{+/-}$ female mice (n=6) were superovulated with 5 IU of pregnant mare serum and 48–50 hours later with 5 IU of human chorionic gonadotropin. Immediately following injections, female mice were mated to heterozygous male mice. Embryos were harvested at different time points. Genomic DNA was isolated from fetal membranes or whole embryos from E4.5, E9.5 and E15.5 and genotyping was performed by PCR based method as described above.

Pgm2 Activity Assay

Pgm2 enzyme activity in fibroblasts and tail clips were measured as described previously by Tegtmeyer and coworkers (Tegtmeyer et al. 2014).

Western Blot Analysis

The tissue samples were collected from age and sex matched wild type and *Pgm2* $^{+/-}$ mice and the expression of Pgm2 protein was analyzed by Western Blot analysis. Briefly, the frozen tissues were homogenized in ice-cold hypotonic lysis buffer (1 mM EDTA, 10 mM Tris-HCl, pH 7.4), supplemented with protease inhibitor cocktail (1 mg/ml each of aprotinin, pepstatin, and leupeptin; 100 mg/ml phenylmethyl sulfonyl fluoride and 2 mM sodium orthovanadate). Homogenized samples were centrifuged at 18,000 × g at 4 °C for 20 min and the supernatant was collected. Protein concentrations were determined by a BCA Protein assay kit (Thermo Scientific, Product # 23223) using a microplate reader. 40 μg of the total protein was resolved by 12 % SDS-PAGE before being transferred to a nitrocellulose membrane. Rabbit anti-human PGM1 antibody (Sigma Aldrich, St. Louis, MO, cat # HPA024190) was used as the primary antibody to detect the mouse Pgm2 protein. Primary antibody was detected with IR dye-conjugated secondary antibodies and visualized by Odyssey Image Analyzer (Li-Cor Biotechnology, Lincoln, NE). The abundance of Pgm2 protein in each sample was normalized to the corresponding Gapdh (Sigma Aldrich, St. Louis, MO, cat # G9545) abundance detected from the same blot.

Galactose rescue experiments in animals

Galactose rescue experiments were performed by oral supplementation of sterile filtered galactose (9mg/ml in drinking water) to the adult females one week before mating and during the course of pregnancies.

Glycome Analysis

Glycome analysis of intact transferrin in serum and fibroblasts was conducted using MALDI-TOF mass spectrometry as previously described (Ferreira et al. 2018). For transferrin analysis, blood was collected from three age- and sex- matched wild type and *Pgm2*$^{+/-}$ animals, respectively and sera were collected after clotting. For fibroblast analysis, skin fibroblasts isolated from two age-, sex- matched wild type and *Pgm2*$^{+/-}$ animals were used to establish primary cell strains, which were used for subsequent analysis.

Results

Construction of the new Pgm2-KO mouse model

Similar to humans, mice have multiple Pgm isoforms (Pgm1, Pgm2 and Pgm3) with distinct substrate specificities (Shows, Ruddle, and Roderick 1969). The murine *Pgm2* gene encodes an enzyme that belongs to the phosphohexose mutase family and catalyzes the bidirectional interconversion of glucose-1-phosphate (Glc-1P) and glucose-6-phosphate (Glc-6P). The mouse Pgm1, on the other hand, catalyzes the conversion of the nucleoside breakdown of ribose-1-phosphate or deoxyribose-1-phosphate to the corresponding 5-phosphopentose. Similar to human PGM3, the mouse Pgm3 facilitates the conversion of *N*-acetyl-glucosamine-6-phosphate (GlcNAc-6-P) to *N*-acetyl-d-glucosamine-1-phosphate (GlcNAc-1-P) (Greig et al. 2007; Muenks, Stiers, and Beamer 2017; Stray-Pedersen et al. 2014; Konno, Niwa, and Yasumura 1989). Based upon published substrate activities, the mouse Pgm2 enzyme is the equivalent of the human PGM1. To further substantiate this claim, we compared the amino acid sequences encoded by different mouse *Pgm* genes to that of human PGM1. Fig. 2a shows that out of 562 amino acids, the mouse Pgm2 protein shares an identity of 97.7% (549 a.a. identical). At the cDNA level, *Pgm2* cDNA (NM_028132) is 90.11% identical to its human counterpart (data not shown). Since Exons 2 and 3 encode residues that make up the active site and substrate binding site, respectively (Stiers et al. 2016), we designed CRISPR reagents that target both exons.

Two pups (one male and one female) born to a pseudopregnant female mouse were tested positive for the disruption of exons 2 & 3 by High Resolution Melting Analysis (HRMA) (data not shown). These mice were crossed to wild-type animals to establish founder animals, which were later crossed to wild type mice to confirm germline transmission. DNA sequencing revealed an insertion/deletion mutation (c.[293_298insAC;293delCGTA]) and a deletion mutation (c.482delTGACT) in exons 2 and 3, respectively (Fig. 2b). The CRISPR reagent that targets exon 2 introduced an insertion-deletion frameshift mutation at the GCC codon encoding amino acid alanine 98 (Ala-98) (Fig. 2b), which led to the creation of a premature stop codon (TAA) 60 nucleotides downstream, and eliminated the serine −117 at the active site (Beamer 2015) in the process. The CRISPR reagent that targets exon 3 led to a frameshift and the creation of a premature stop codon (TGA) 38 nucleotides downstream.

Molecular Genotyping of Pgm2-KO allele

The insertion-deletion mutation introduced in Exon 2 ablates a *BceAI* restriction site. Using PCR primers described in Materials and Methods above, we were able to amplify a PCR product of 788 bp from the wild-type allele. *BceA*I restriction digestion resulted in two

fragments (504 bp and 284 bp) and was used to distinguish between the mutant and wild type alleles (Fig. 2c)

Embryonic Lethality in homozygotes

Hoping to obtain homozygotes for further studies, we set up crosses between heterozygous parents. After analyzing more than 70 pups from over 10 crosses, we were unable to identify *Pgm2*$^{-/-}$ homozygotes (p = 1.59897E-06) (Table 1). This suggested embryonic lethality. Moreover, we found four of the heterozygous pups, but none of the wild type, died within two days after birth.

To assess the approximate time at which Pgm2-deficient embryos succumb *in utero*, we conducted ultrasound studies on pregnant heterozygous female mice mated with heterozygous males throughout the gestation period. We monitored six pregnancies and our results indicated almost all pregnancies had nine or more living embryos to start with, but two or three embryos from each litter began to show arrested development at around E9.5 (Fig. 3). Molecular genotyping of the dissected embryos from the euthanized dams confirmed that embryos succumbed were homozygotes (see Fig. 2c). Three of the dead embryos were found to be heterozygotes, but none were wild-type. We also conducted timed mating experiments to reinforce the results of the ultrasound studies. In this case, we followed up to six separate pregnancies. Two pregnant dams were euthanized and dissected at day E4.5. Two were euthanized and dissected at E9.5 and the other two were euthanized and dissected at E15.5. Similar to what we found in the ultrasound work, 8–10 embryos were seen in all pregnancies as revealed from pregnant dams euthanized at E4.5 (Supplementary Fig. 1), but some of the embryos became arrested shortly before E9.5 (Supplementary Fig. 1). Molecular genotyping confirmed the dead embryos in six pregnancies were homozygotes, as well as four heterozygotes.

We also attempted to rescue the lethality phenotype by oral galactose supplementation based upon the dosage used in human patients (Tegtmeyer et al. 2014; Wong et al. 2017), but we observed no effects at the dosing regimen we employed (Table 1).

Biochemical Studies of heterozygous Pgm2$^{+/-}$ animals and cells

Since we could not obtain any homozygous *Pgm2*$^{-/-}$ livebirths, we confirmed the knockout of the *Pgm2* gene in the heterozygous animals by measuring the Pgm2 activity in their skin fibroblasts and tissues (tail clips). Fig. 4a & b showed significant (more than 60%) reduction of Pgm2 activity in the fibroblasts and tail clips in the heterozygous animals, which was reflected in the Western Blot analysis of the corresponding tail clip samples (Fig. 4c).

Glycome Analysis

Glycoprofiling in PGM1 deficiency in humans shows a recognizable pattern with changes in three glycan indexes (1. normal glycosylation, 2. lack of complete glycans, and 3. lack of galactose residues), with decrease in total galactosylation and sialylation. There is also frequently an increase in high mannose glycans and fucosylation of total plasma glycans (Abu Bakar et al. 2018).

Our glycomics studies in heterozygous *Pgm2*$^{+/-}$ mice showed a distinct glycosylation pattern compared to the glycosylation pattern in wild type mice, but different from the human PGM1 deficient pattern. In the serum analysis of intact transferrin in heterozygous *Pgm2*$^{+/-}$ mice there was a profound decrease of the tetrasialotransferrin glycoform (type I), and a relative increase of truncated glycans (type II pattern) (Fig. 5). (Please note that mice serum has a relative increase in truncated glycans in wild type mice, compared to healthy human serum). The MALDI-TOF analysis of total glycans of in heterozygous *Pgm2*$^{+/-}$ mice serum showed no abnormalities. There was some difference in the global galactosylation pattern with increased presence of total ungalactosylated truncated glycans in heterozygous *Pgm2*$^{+/-}$ mice, and there was no terminal sialylation observed in the heterozygous fibroblasts, similar to the pattern seen in human fibroblasts. However, there was no increase in mannosylation and fucosylation. No apparent loss-of-glycans were detected. These changes suggest a glycan-processing defect in heterozygotes, but different from biallelic *PGM1* mutant cells in humans.

Discussion

To understand the pathophysiology of PGM1 deficiency and to facilitate the development of novel therapeutics, we here report the construction of a constitutive *Pgm2*-KO mouse model using CRISPR-Cas9 technology (Fig. 2). By comparing the amino acid sequences of different isoforms to the human PGM1, we confirmed that the mouse Pgm2 protein shares the highest identity with human *PGM1* (Fig. 2a) and therefore, we chose to target the *Pgm2* gene in this study. The insertion/deletion at exon 2 and the deletion mutation in exon 3 each create a premature stop codon in the respective exon by itself. In addition, both mutations led to frameshifts alone or in combination. Therefore, the chance for a functional Pgm2 protein to be produced through single/double read-throughs is virtually non-existent.

In this study, we demonstrated that homozygosity for *Pgm2*-KO mutations leads to embryonic lethality in mice (Table 1, Figs.3 & Supplementary Fig. 1). While other mouse models of CDG, such as *Pmm2*-KO mice, also exhibited lethality for the homozygous embryos, our Pgm2-deficient model presents some differences (Thiel et al. 2006; DeRossi et al. 2006). As to the *Pmm2*-KO mouse, no *Pmm2*-null embryos were recovered beyond the embryonic day 3.5 (Thiel et al. 2006). Yet, our Pgm2-deficient embryos appeared to perish shortly before E9.5 (Fig. 3, Supplementary Fig. 1). Could this be due to the existence of multiple Pgm isoforms which partially compensate for the loss of Pgm2 activity and sustain embryonic development till mid-gestation when organogenesis begins when the demand for Pgm2 function is so critical that even the other isoforms are insufficient? Regardless, we can conclude that no protein in the mouse that compensates for Pgm2 for survival. At the moment, it is unclear why the KO animals perish *in utero*. Tamplin and coworkers showed that *Pgm2* is expressed abundantly in the heart around E8.5 (Tamplin et al. 2008).

Surprisingly, some *Pgm2*$^{+/-}$ embryos did not come to full term either, while we did not see any deaths of wild type embryos throughout our studies. In addition, 7% of heterozygous newborns died soon after birth. This suggests that *Pgm2*$^{+/-}$ mice are seemingly more affected than heterozygous patients, but it should be noted that there are no formal retrospective or longitudinal studies of the human carriers. Remarkably, when we assessed

the Pgm2 enzymatic activity in the tissues or cultured skin fibroblasts from the surviving *Pgm2*$^{+/-}$animals, we revealed more than 60% reduction in enzymatic activity, with a few in the 30–40% range. Could the unusually low Pgm2 activity in the heterozygous animals, which potentially can be treated like human symptomatic patients who harbor hypomorphic mutations, explain their worse-than-expected phenotypes? While it is beyond the scope of the current work to investigate the mechanisms that account for the lower than expected Pgm2 activity in the heterozygotes, but we will examine any potential dominant negative effect of the heterozygous KO mutation, as well as other potential epigenetic mechanisms in the future.

The pathological condition in the heterozygous animals was also reflected in the abnormal glycosylation studies of the serum transferrin and skin fibroblasts harvested from heterozygous animals. In both cases, mass spectrometry showed increased levels of truncated glycans with decreased galactosylation (Fig 5 and Supplementary Fig. 2), which is one of the characteristic features in human PGM1-CDG patients carrying biallelic mutations (Wong et al. 2017; Witters, Cassiman, and Morava 2017). Therefore, our heterozygous mouse model mirrors an important aspect of the human phenotype. These heterozygous mice also showed loss of serum glycans, which is the other diagnostic feature of PGM1-deficient patients. Therefore, our findings suggest that a significant reduction of Pgm2 activity in the carrier cells is sufficient to cause both type I and type II glycosylation defects in the Golgi.

Schneider and colleagues reported that mannose supplementation rescued the embryonic lethality phenotype in the *Pmm2*$^{R137H/F118L}$ model (Schneider et al. 2011), but Chan and coworkers were unsuccessful in their attempt with the same amount of mannose in *Pmm2*$^{R137H/F115L}$ model, which showed 62% embryonic lethality in homozygotes. However, they were able to significantly rescue embryonic lethality in the *Pmm2*$^{F115L/F115L}$ homozygous mutants (Chan et al. 2016). Nonetheless, Wong and colleagues were able to reverse some of the biochemical phenotypes of PGM1 deficiency in human patients and cells with hypomorphic mutations, despite the fact that not all phenotypes were corrected (Morava 2014; Wong et al. 2017). Therefore, we examined effects of galactose supplementation at 9mg/ml (drinking water) based upon the dosage used in human patients (1.5g/kg/day), but were unable to correct any mouse phenotype, in particular the reversal of embryonic lethal phenotype of the homozygotes (Table 1). In hindsight, our hope for rescue might be over-ambitious because after all, ours is a complete KO mouse model *versus* a hypomorphic human one. We can conclude that even under galactose treatment, no other enzyme can take over the role of Pgm2. We will also evaluate the effects of galactose supplementation on other biochemical markers in the heterozygous (hypomorphic) mutants.

Supplementary Material

Refer to Web version on PubMed Central for supplementary material.

Acknowledgement

Research support include the Primary Children's Hospital Foundation K2R2R Award (to KL), UDN Metabolomics Core and FP00096621 (National Center for Advancing Translational Sciences) grants (to EM), and NIH S10 RR027506–01 grant awarded to KJW at the University of Utah Small Animal Ultrasound Core.

Details of funding

Research support include the Primary Children's Hospital Foundation K2R2R Award (to KL), UDN Metabolomics Core and FP00096621 (National Center for Advancing Translational Sciences) grants (to EM), and NIH grant S10 RR027506–01 awarded to the University of Utah Small Animal Ultrasound Core Facility.

Name of one author who serves as guarantor

Kent Lai

References

Abu Bakar N, Voermans NC, Marquardt T, Thiel C, Janssen MCH, Hansikova H, Crushell E, Sykut-Cegielska J, Bowling F, Orkrid LM, Vissing J, Morava E, van Scherpenzeel M, and Lefeber DJ. 2018 'Intact transferrin and total plasma glycoprofiling for diagnosis and therapy monitoring in phosphoglucomutase-I deficiency', Transl Res, 199: 62–76. [PubMed: 30048639]

Beamer L 2015 'Mutations in hereditary phosphoglucomutase 1 deficiency map to key regions of enzyme structure and function', Journal of Inherited Metabolic Disease, 38: 243–56. [PubMed: 25168163]

Chan B, Clasquin M, Smolen GA, Histen G, Powe J, Chen Y, Lin ZZ, Lu CM, Liu Y, Cang Y, Yan ZH, Xia YF, Thompson R, Singleton C, Dorsch M, Silverman L, Su SS, Freeze HH, and Jin SF. 2016 'A mouse model of a human congenital disorder of glycosylation caused by loss of PMM2', Human Molecular Genetics, 25: 2182–93. [PubMed: 27053713]

DeRossi C, Bode L, Eklund EA, Zhang FR, Davis JA, Westphal V, Wang L, Borowsky AD, and Freeze HH. 2006 'Ablation of mouse phosphomannose isomerase (Mpi) causes mannose 6-phosphate accumulation, toxicity, and embryonic lethality', Journal of Biological Chemistry, 281: 5916–27. [PubMed: 16339137]

Ferreira CR, Xia ZJ, Clement A, Parry DA, Davids M, Taylan F, Sharma P, Turgeon CT, Blanco-Sanchez B, Ng BG, Logan CV, Wolfe LA, Solomon BD, Cho MT, Douglas G, Carvalho DR, Bratke H, Haug MG, Phillips JB, Wegner J, Tiemeyer M, Aoki K, Network Undiagnosed Diseases, Partnership Scottish Genome A Nordgren A Hammarsjo AL Duker L Rohena HB Hove J Ek D Adams CJ Tifft T Onyekweli T Weixel E Macnamara K Radtke Z Powis D Earl M Gabriel AHS Russi L Brick M Kozenko E Tham KM Raymond JA Phillips GE Tiller WG Wilson R Hamid MCV Malicdan G Nishimura G Grigelioniene A Jackson M Westerfield MB Bober WA Gahl, and Freeze HH 2018 'A Recurrent De Novo Heterozygous COG4 Substitution Leads to Saul-Wilson Syndrome, Disrupted Vesicular Trafficking, and Altered Proteoglycan Glycosylation', Am J Hum Genet, 103: 553–67. [PubMed: 30290151]

Greig KT, Antonchuk J, Metcalf D, Morgan PO, Krebs DL, Zhang JG, Hacking DF, Bode L, Robb L, Kranz C, de Graaf C, Bahlo M, Nicola NA, Nutt SL, Freeze HH, Alexander WS, Hilton DJ, and Kile BT. 2007 'Agm1/Pgm-3-mediated sugar nucleotide synthesis is essential for hematopoiesis and development', Molecular and Cellular Biology, 27: 5849–59. [PubMed: 17548465]

Jaeken J 2011 'Congenital disorders of glycosylation (CDG): it's (nearly) all in it!', Journal of Inherited Metabolic Disease, 34: 853–58. [PubMed: 21384229]

Konno R, Niwa A, and Yasumura Y. 1989 'Linkage of the Dao-1 Gene for D-Amino-Acid Oxidase to the Pgm-1 Gene for Phosphoglucomutase-1 on the Mouse Chromosome-5', Japanese Journal of Genetics, 64: 341–45. [PubMed: 2576634]

Kucukcongar A, Tumer L, Ezgu FS, Kasapkara CS, Jaeken J, Matthijs G, Rymen D, Dalgic B, Bideci A, and Hasanoglu A. 2015 'A Case with Rare Type of Congenital Disorder of Glycosylation: Pgm1-Cdg', Genetic Counseling, 26: 87–90. [PubMed: 26043514]

Lin S, Staahl B, Alla RK, and Doudna JA. 2014 'Enhanced homology-directed human genome engineering by controlled timing of CRISPR/Cas9 delivery', Elife,3

Loewenthal N, Haim A, Parvari R, and Hershkovitz E. 2015 'Phosphoglucomutase-1 Deficiency: Intrafamilial Clinical Variability and Common Secondary Adrenal Insufficiency', American Journal of Medical Genetics Part A, 167: 3139–43.

Morava E 2014 'Galactose supplementation in phosphoglucomutase-1 deficiency; review and outlook for a novel treatable CDG', Molecular Genetics and Metabolism, 112: 275–79. [PubMed: 24997537]

Muenks AG, Stiers KM, and Beamer LJ. 2017 'Sequence-structure relationships, expression profiles, and disease-associated mutations in the paralogs of phosphoglucomutase 1', PLoS One, 12.

Ondruskova N, Honzik T, Vondrackova A, Tesarova M, Zeman J, and Hansikova H. 2014 'Glycogen storage disease-like phenotype with central nervous system involvement in a PGM1-CDG patient', Neuroendocrinology Letters, 35: 137–41. [PubMed: 24878975]

Perez B, Medrano C, Ecay MJ, Ruiz-Sala P, Martinez-Pardo M, Ugarte M, and Perez-Cerda C. 2013 'A novel congenital disorder of glycosylation type without central nervous system involvement caused by mutations in the phosphoglucomutase 1 gene', Journal of Inherited Metabolic Disease, 36: 535–42. [PubMed: 22976764]

Radenkovic S, Bird MJ, Emmerzaal TL, Wong SY, Felgueira C, Stiers KM, Sabbagh L, Himmelreich N, Poschet G, Windmolders P, Verheijen J, Witters P, Altassan R, Honzik T, Eminoglu TF, James PM, Edmondson AC, Hertecant J, Kozicz T, Thiel C, Vermeersch P, Cassiman D, Beamer L, Morava E, and Ghesquiere B. 2019 'The Metabolic Map into the Pathomechanism and Treatment of PGM1-CDG', Am J Hum Genet.

Schneider A, Theil C, Rindermann J, DeRossi C, Popovici D, Hoffmann GF, Grone HJ, and Korner C. 2011 'Successful prenatal mannose treatment for congenital disorder of glycosylation-Ia in mice.', Nat Med, 18: 71–83. [PubMed: 22157680]

Shows TB, Ruddle FH, and Roderick TH. 1969 'Phosphoglucomutase Electrophoretic Variants in Mouse', Biochemical Genetics, 3: 25-&.

Stiers KM, Kain BN, Graham AC, and Beamer LJ. 2016 'Induced Structural Disorder as a Molecular Mechanism for Enzyme Dysfunction in Phosphoglucomutase 1 Deficiency', Journal of Molecular Biology, 428: 1493–505. [PubMed: 26972339]

Stojkovic T, Vissing J, Petit F, Piraud M, Orngreen MC, Andersen G, Claeys KG, Wary C, Hogrel JY, and Laforet P. 2009 'Muscle Glycogenosis Due to Phosphoglucomutase 1 Deficiency', New England Journal of Medicine, 361: 425–27. [PubMed: 19625727]

Stray-Pedersen A, Backe PH, Sorte HS, Morkrid L, Chokshi NY, Erichsen HC, Gambin T, Elgstoen KBP, Bjoras M, Wlodarski MW, Kruger M, Jhangiani SN, Muzny DM, Patel A, Raymond KM, Sasa GS, Krance RA, Martinez CA, Abraham SM, Speckmann C, Ehl S, Hall P, Forbes LR, Merckoll E, Westvik J, Nishimura G, Rustad CF, Abrahamsen TG, Ronnestad A, Osnes LT, Egeland T, Rodningen OK, Beck CR, Boerwinkle EA, Gibbs RA, Lupski JR, Orange JS, Lausch E, Hanson IC, and Baylor-Johns Hopkins Ctr Mendelian. 2014 'PGM3 Mutations Cause a Congenital Disorder of Glycosylation with Severe Immunodeficiency and Skeletal Dysplasia', American Journal of Human Genetics, 95: 96–107. [PubMed: 24931394]

Tamplin OJ, Kinzel D, Cox BJ, Bell CE, Rossant J, and Lickert H. 2008 'Microarray analysis of Foxa2 mutant mouse embryos reveals novel gene expression and inductive roles for the gastrula organizer and its derivatives', Bmc Genomics, 9.

Tegtmeyer LC, Rust S, van Scherpenzeel M, Ng BG, Losfeld ME, Timal S, Raymond K, He P, Ichikawa M, Veltman J, Huijben K, Shin YS, Sharma V, Adamowicz M, Lammens M, Reunert J, Witten A, Schrapers E, Matthijs G, Jaeken J, Rymen D, Stojkovic T, Laforet P, Petit F, Aumaitre O, Czarnowska E, Piraud M, Podskarbi T, Stanley CA, Matalon R, Burda P, Seyyedi S, Debus V, Socha P, Sykut-Cegielska J, van Spronsen F, de Meirleir L, Vajro P, DeClue T, Ficicioglu C, Wada Y, Wevers RA, Vanderschaeghe D, Callewaert N, Fingerhut R, van Schaftingen E, Freeze HH, Morava E, Lefeber DJ, and Marquardt T. 2014 'Multiple Phenotypes in Phosphoglucomutase 1 Deficiency', New England Journal of Medicine, 370: 533–42. [PubMed: 24499211]

Thiel C, Lubke T, Matthijs G, von Figura K, and Korner C. 2006 'Targeted disruption of the mouse phosphomannomutase 2 gene causes early embryonic lethality', Molecular and Cellular Biology, 26: 5615–20. [PubMed: 16847317]

Timal S, Hoischen A, Lehle L, Adamowicz M, Huijben K, Sykut-Cegielska J, Paprocka J, Jamroz E, van Spronsen FJ, Korner C, Gilissen C, Rodenburg RJ, Eidhof I, Van den Heuvel L, Thiel C,

Wevers RA, Morava E, Veltman J, and Lefeber DJ. 2012 'Gene identification in the congenital disorders of glycosylation type I by whole-exome sequencing', Human Molecular Genetics, 21: 4151–61. [PubMed: 22492991]

Voermans NC, Preisler N, Madsen KL, Janssen MCH, Kusters B, Abu Bakar N, Conte F, Lamberti VML, Nusman F, van Engelen BG, van Scherpenzeel M, Vissing J, and Lefeber DJ. 2017 'PGM1 deficiency: Substrate.use during exercise and effect of treatment with galactose', Neuromuscular Disorders, 27: 370–76. [PubMed: 28190645]

Witters P, Cassiman D, and Morava E. 2017 'Nutritional Therapies in Congenital Disorders of Glycosylation (CDG)', Nutrients, 9.

Wong SYW, Gadomski T, van Scherpenzeel M, Honzik T, Hansikova H, Holmefjord KSB, Mork M, Bowling F, Sykut-Cegielska J, Koch D, Hertecant J, Preston G, Jaeken J, Peeters N, Perez S, Do Nguyen D, Crivelly K, Emmerzaal T, Gibson KM, Raymond K, Abu Bakar N, Foulquier F, Poschet G, Ackermann AM, He M, Lefeber DJ, Thiel C, Kozicz T, and Morava E. 2017 'Oral D-galactose supplementation in PGM1-CDG', Genetics in Medicine, 19: 1226–35. [PubMed: 28617415]

Synopsis

Mice deficient in Phosphoglucomutase 2 (Pgm2) activity exhibit aberrant glycosylation and embryonic lethality.

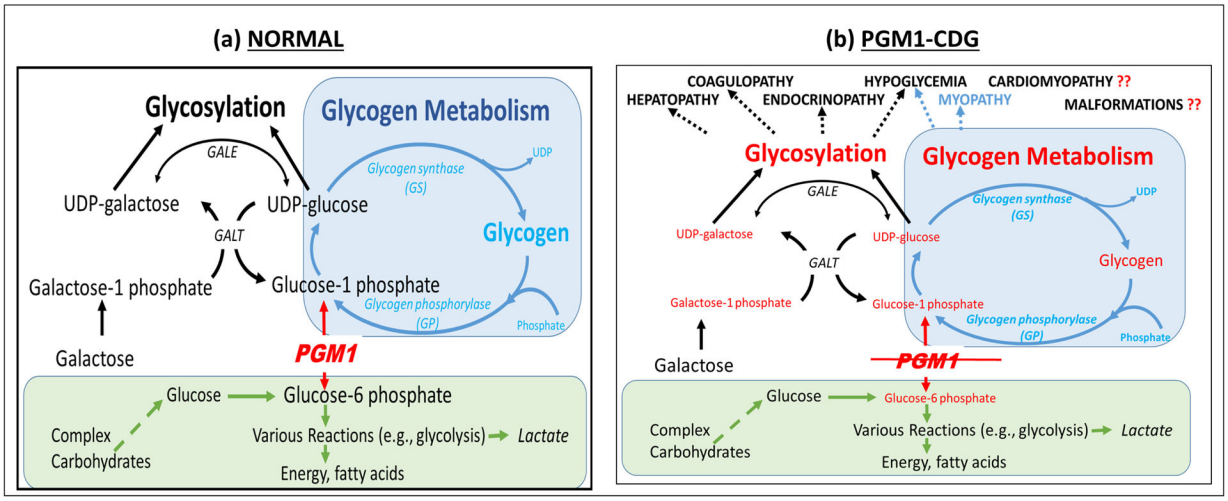

Fig. 1. Multi-system involvement in human PGM1-CDG.

(a) PGM1 catalyzes the interconversion of glucose-1 phosphate and glucose-6 phosphate) and therefore, it plays a regulatory role in glycolysis, glycogenesis, glycogenolysis, and glycosylation. (b) PGM1 deficiency (PGM1-CDG) leads to fasting hypoglycemia, but under normal feeding conditions, there is significant decrease in UDP-glucose and UDP-galactose levels, as well as glucose-1 phosphate and galactose-1 phosphate. As a result, both glycosylation and glycogen metabolism are perturbed, leading to multi-system dysfunctions. (GALT: galactose-1 phosphate uridylyltransferase, GALE: UDP-galactose-4’ epimerase)

```
                1       10        20        30        40        50        60        70        80        90       100       110       120       130
                |--------+---------+---------+---------+---------+---------+---------+---------+---------+---------+---------+---------+---------|
Human PGM1      MVKIVTVKTQAYQDQKPGTSGLRKRVKVFQSSANYAENFIQSIISTVEPAQRQEATLVYGGDGRFYMKEAIQLIARIAAANGIGRLVIGQNGILSTPAVSCIIRKIKAIGGIILTASHNPGGPNGDFGIK
Mouse Pgm2      MVKIVTVKTQAYPDQKPGTSGLRKRVKVFQSNANYAENFIQSIVSTVEPALRQEATLVYGGDGRFYMTEAIQLIVRIAAANGIGRLVIGQNGILSTPAVSCIIRKIKAIGGIILTASHNPGGPNGDFGIK
Consensus       MVKIVTVKTQAYqDQKPGTSGLRKRVKVFQSnANYAENFIQSI!STVEPAqRQEATLVYGGDGRFYMkEAIQLIaRIAAANGIGRLVIGQNGILSTPAVSCIIRKIKAIGGIILTASHNPGGPNGDFGIK

                131     140       150       160       170       180       190       200       210       220       230       240       250       260
                |--------+---------+---------+---------+---------+---------+---------+---------+---------+---------+---------+---------+---------|
Human PGM1      FNISNGGPAPEAITDKIFQISKTIEEYAVCPDLKVDLGVLGKQQFDLENKFKPFTVEIVDSVEAYATMLRSIFDFSALKELLSGPNRLKICIDAMHGVVGPYVKKILCEELGAPANSAVNCVPLEDFGGH
Mouse Pgm2      FNISNGGPAPEAITDKIFQISKTIEEYAICPDLKVDLGVLGKQQFDLENKFKPFTVEIVDSVEAYATMLRNIFDFNALKELLSGPNRLKIRIDAMHGVVGPYVKKILCEELGAPANSAVNCVPLEDFGGH
Consensus       FNISNGGPAPEAITDKIFQISKTIEEYA!CPDLKVDLGVLGKQQFDLENKFKPFTVEIVDSVEAYATMLRnIFDFnALKELLSGPNRLKIrIDAMHGVVGPYVKKILCEELGAPANSAVNCVPLEDFGGH

                261     270       280       290       300       310       320       330       340       350       360       370       380       390
                |--------+---------+---------+---------+---------+---------+---------+---------+---------+---------+---------+---------+---------|
Human PGM1      HPDPNLTYAADLVETMKSGEHDFGAAFDGDGDRNMILGKHGFFVNPSDSVAVIAANIFSIPYFQQTGVRGFARSMPTSGALDRVASATKIALYETPTGWKFFGNLMDASKLSLCGEESFGTGSDHIREKD
Mouse Pgm2      HPDPNLTYAADLVETMKSGEHDFGAAFDGDGDRNMILGKHGFFVNPSDSVAVIAANIFSIPYFQQTGVRGFARSMPTSGALDRVANATKIALYETPTGWKFFGNLMDASKLSLCGEESFGTGSDHIREKD
Consensus       HPDPNLTYAADLVETMKSGEHDFGAAFDGDGDRNMILGKHGFFVNPSDSVAVIAANIFSIPYFQQTGVRGFARSMPTSGALDRVAnATKIALYETPTGWKFFGNLMDASKLSLCGEESFGTGSDHIREKD

                391     400       410       420       430       440       450       460       470       480       490       500       510       520
                |--------+---------+---------+---------+---------+---------+---------+---------+---------+---------+---------+---------+---------|
Human PGM1      GLWAVLAWLSILATRKQSVEDILKDHWQKHGRNFFTRYDYEEVEAEGANKMMKDLEALMFDRSFVGKQFSANDKVYTVEKADNFEYSDPVDGSISRNQGLRLIFTDGSRIVFRLSGTGSAGATIRLYIDS
Mouse Pgm2      GLWAVLAWLSILATRKQSVEDILKDHWQKFGRNFFTRYDYEEVEAEGANKMMKDLEALMLDRSFVGKQFSANDKVYTVEKADNFEYSDPVDGSISKNQGLRLIFADGSRIIFRLSGTGSAGATIRLYIDS
Consensus       GLWAVLAWLSILATRKQSVEDILKDHWQKhGRNFFTRYDYEEVEAEGANKMMKDLEALMlDRSFVGKQFSANDKVYTVEKADNFEYSDPVDGSISrNQGLRLIFaDGSRI!FRLSGTGSAGATIRLYIDS

                521     530       540       550       56862
                |--------+---------+---------+---------+-|
Human PGM1      YEKDVAKINQDPQVMLAPLISIALKVSQLQERTGRTAPTVIT
Mouse Pgm2      YEKDVAKINQDPQVMLAPLISIALKVSQLQERTGRTAPTVIT
Consensus       YEKDVAKINQDPQVMLAPLISIALKVSQLQERTGRTAPTVIT
```

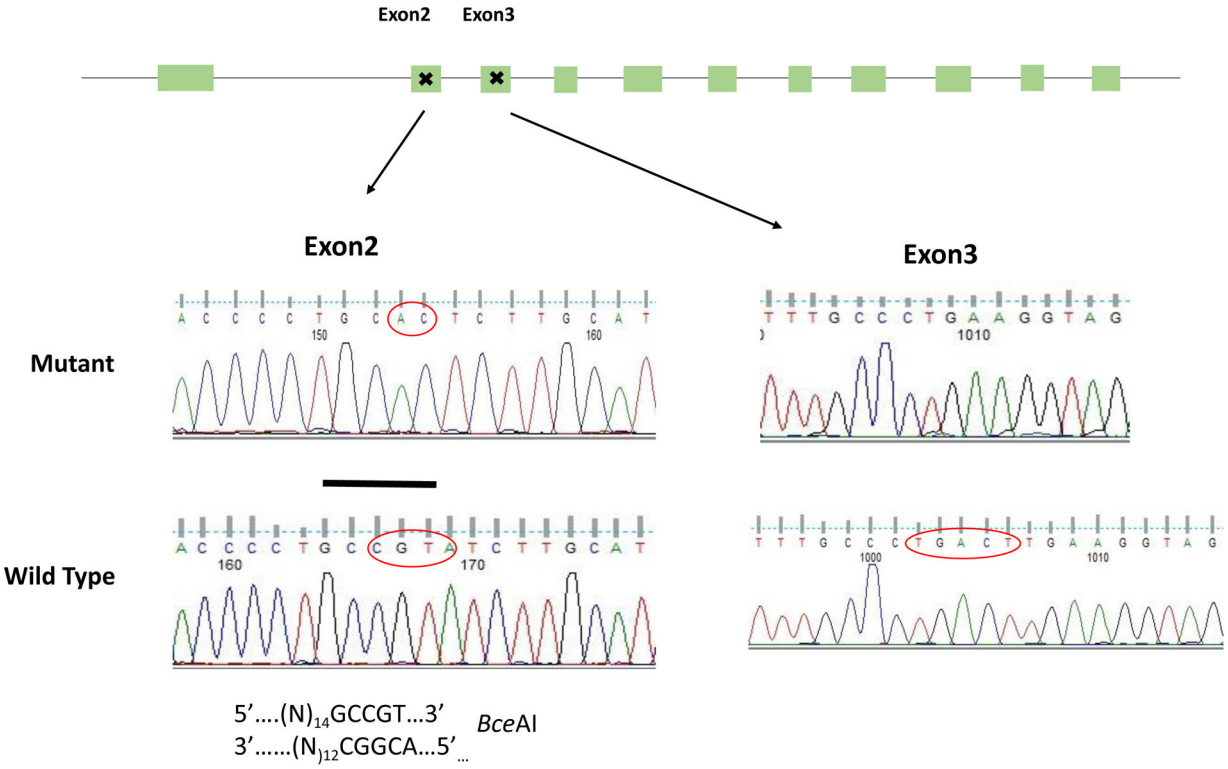

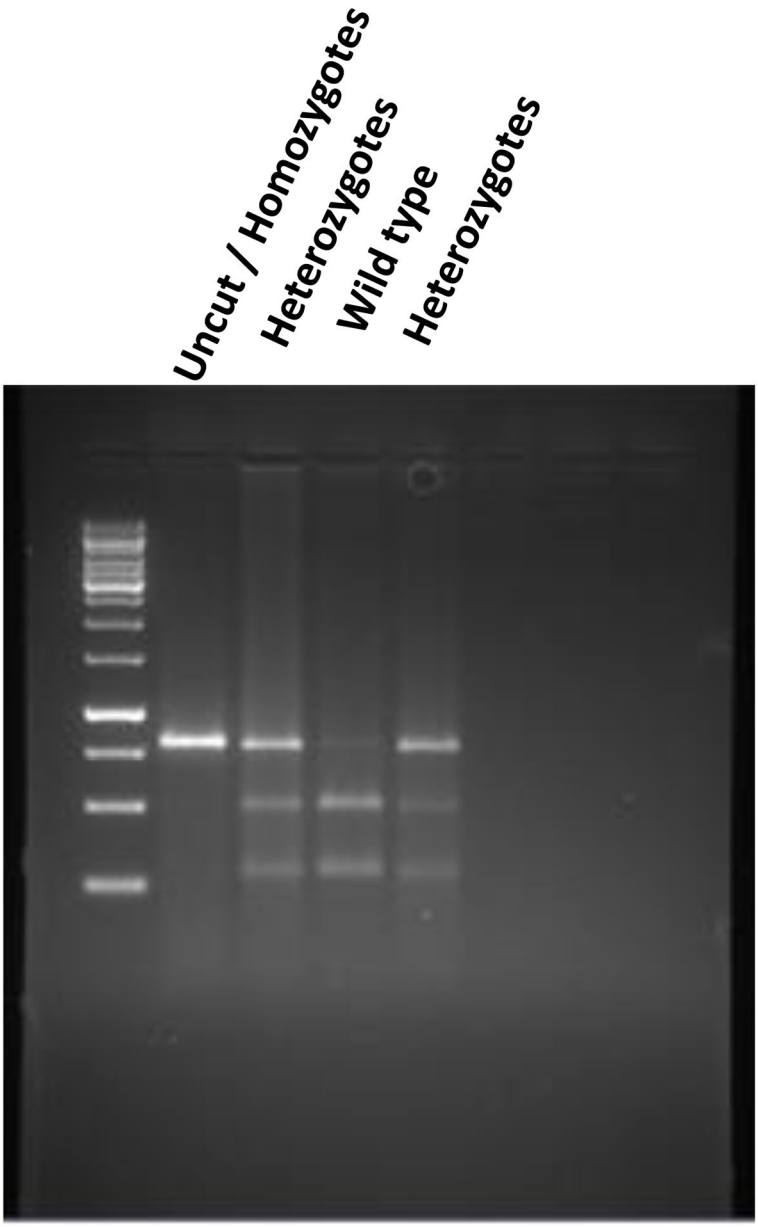

Fig. 2. Construction of traditional Pgm2-KO mice.

a) Amino acid sequences of mouse Pgm2 to that of human PGM1 were compared using *MultAlin* software (http://multalin.toulouse.inra.fr/multalin/). Out of 562 amino acids, the mouse Pgm2 protein share an identity of 97.7% (549 a.a. identical). b) Two CRISPR reagents were used to introduce an insertion-deletion and a deletion, respectively in Exon 2 & 3 of the mouse Pgm2 gene. The frameshift mutation introduced in Exon 2 created a premature stop codon and eliminated a *BceA*I restriction site that was used in PCR-based genotyping. c) Genomic DNA isolated from the mice are amplified by PCR method and digested with restriction endonuclease *BceA*1, producing 788 bp from the uncut or homozygote (lane 2), 788bp, 504 bp and 284 bp from heterozygote (lanes 3 & 5) and 504 bp and 284 bp for the wild-type allele (lane 4).

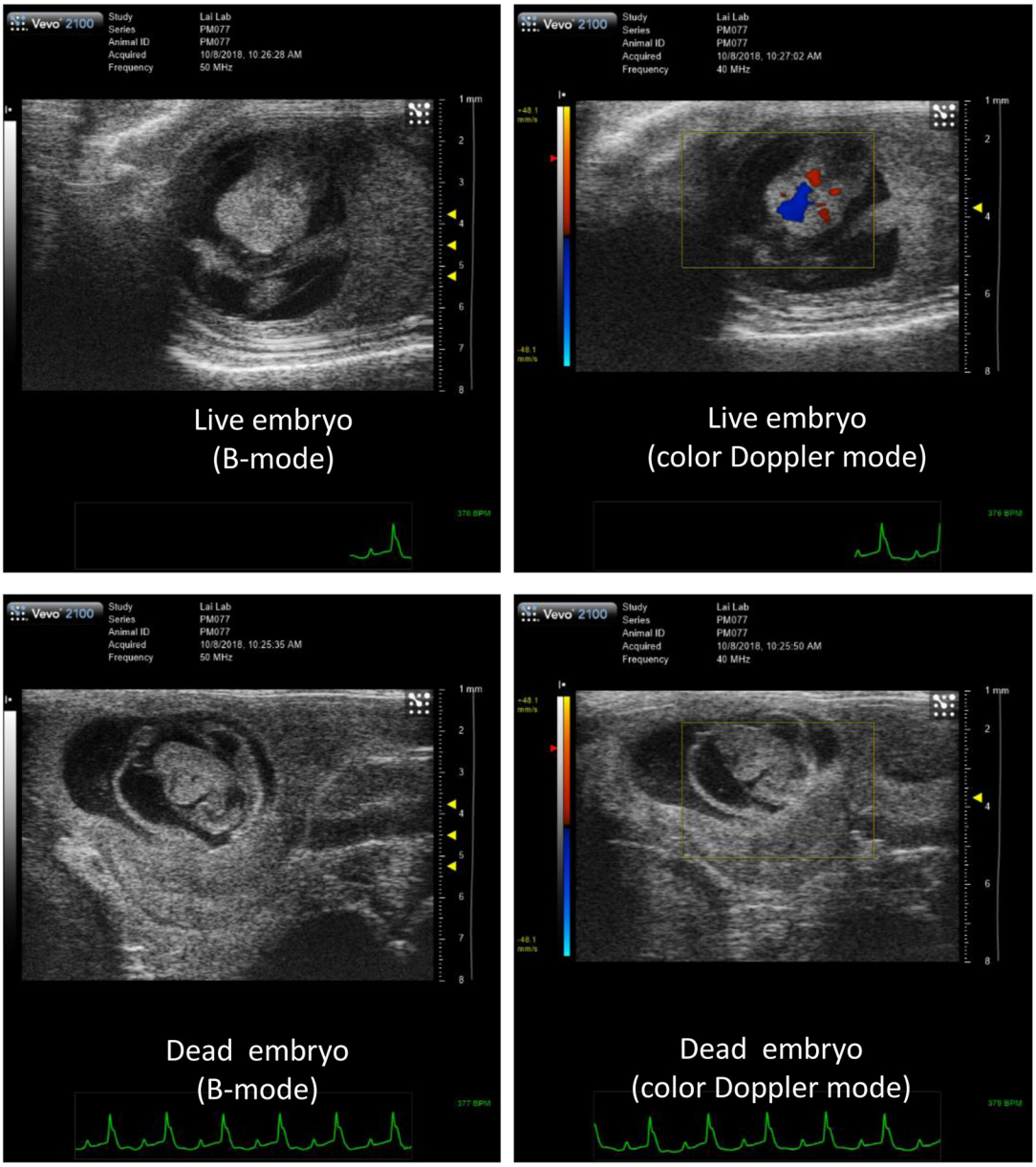

Fig. 3. Use of Ultrasound imaging to follow the course of pregnancies in *Pgm2*$^{+/-}$ females mated to *Pgm2*$^{+-}$ males.

Six pregnancies were followed by ultrasound daily soon after matings began. Color Doppler mode reveals blood flow in the live fetus (upper right panel). The representative figures showed that no blood flow was detected in an E9.5 embryo.

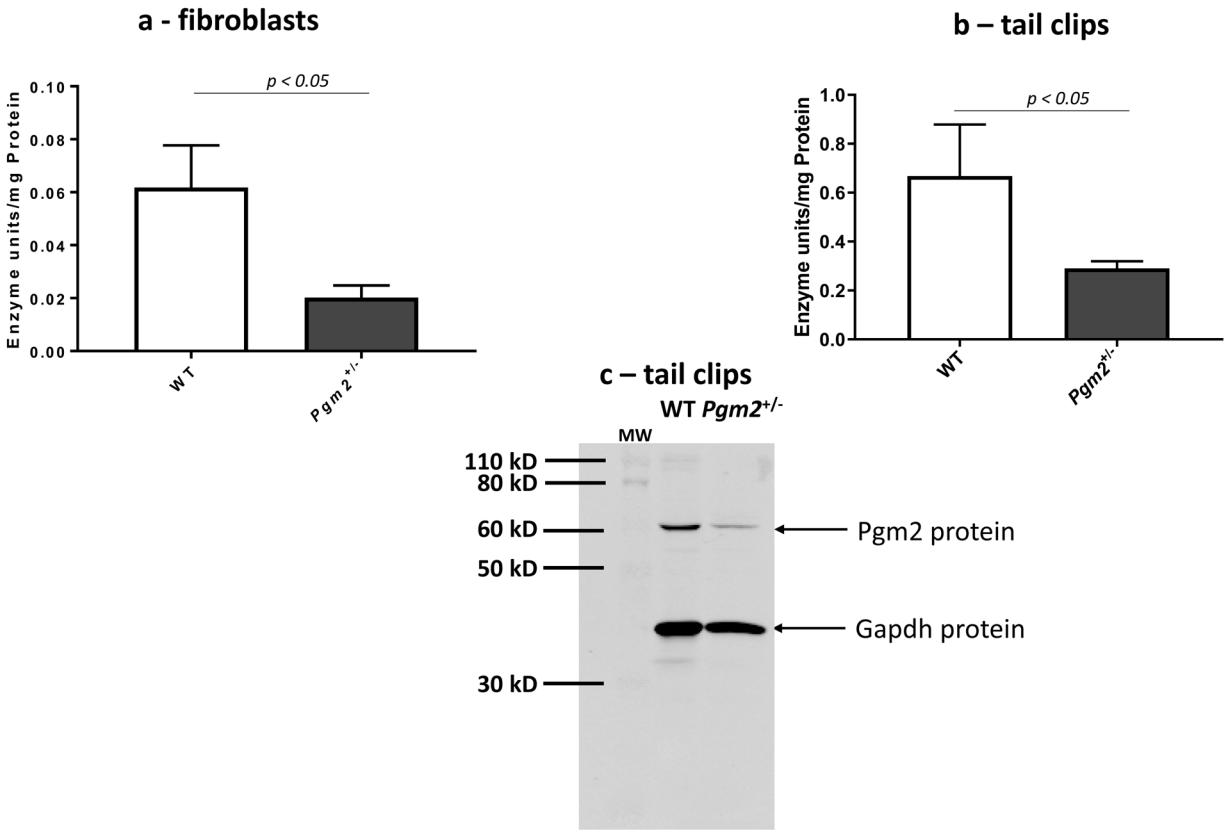

Fig. 4. Biochemical studies of *Pgm2*$^{+/-}$ cells and animals.

Pgm2 activity was determined in (a) skin fibroblasts and (b) tail clips harvested from wild type and heterozygous animals. (c) A representative Western blot analyses of Pgm2 protein abundance in tail clips of wild type and heterozygous animals.

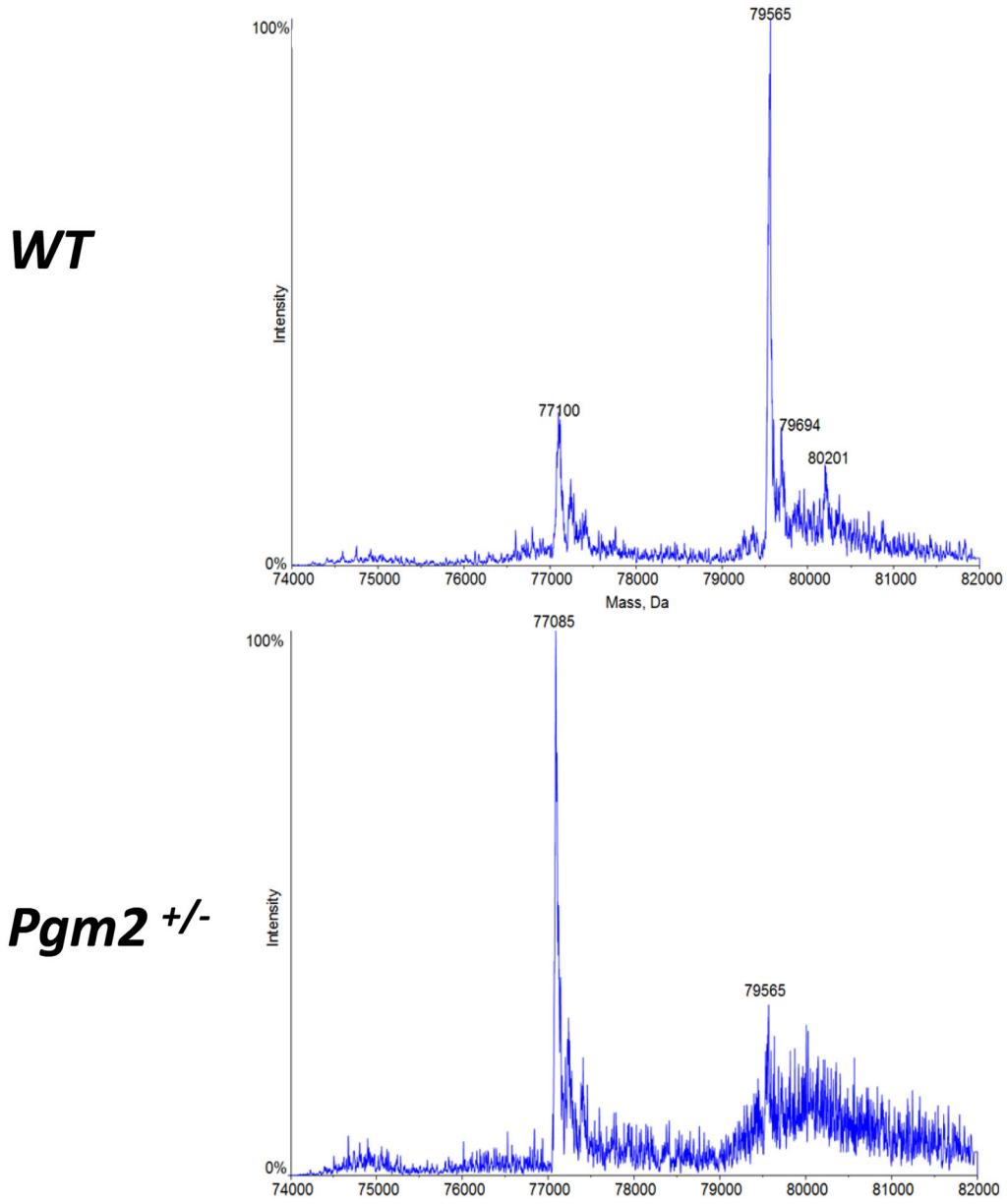

Fig. 5. Abnormal glycosylation of serum transferrin in *Pgm2*$^{+/-}$ heterozygotes.

Representative transferrin spectra in wild type and heterozygous *Pgm2*$^{+/-}$ mice serum evaluated by mass spectrometry. In the heterozygous mice di-oligo (tetrasialo) transferrin was absent and there was a significant increase in the abundance of truncated glycans.

Table 1.

Embryonic Lethality for homozygous *Pgm2*$^{-/-}$ mutants

Galactose supplementation in drinking water	**No**	**Yes**
Number of crosses between het. parents	15	4
Total number of livebirths	78	23
Wild type	23	6
Heterozygotes	55	17
Homozygotes	0	0
Chi square value	26.692	8.39
***p* value**	1.59897E–06	1.5060917E–02